

IL10 and O₃-induced inflammation
Backus GS et al.

Supplemental Materials

Table of Contents

Histological analysis.....	1
Real-time quantitative reverse transcriptase-polymerase chain reaction (qRT-PCR).....	1
Western blot analysis.....	1
Enzyme-linked immunosorbant assay (ELISA) for MIP-2 and p65 NF- κ B.....	1
Nuclear protein isolation and electrophilic mobility shift assay (EMSA) for NF- κ B.....	2
RNA protein isolation and microarray hybridization.....	2
Gene expression analysis.....	3
<i>Selection of profiles to use as seeds for similarity searches.....</i>	4
<i>Similarity searches and results.....</i>	5
<i>Identification of responsive genes.....</i>	6
<i>Pathway identification of genes with responsive profiles.....</i>	6
<i>Analysis of microarray data using GeneSpring.....</i>	7
Reference.....	8
Supplemental material Tables 1-4.....	9-12
Supplemental material Figures 1-7.....	13-26

Histological analysis. We inflated lavaged right lungs with 10% formalin, removed *en bloc*, and immersed the lungs in 10% formalin. After 24 hr, we cut lungs into three cross sections, and processed the sections for histochemical and immunohistochemical analysis. We used hematoxylin and eosin (H&E)-stained tissue sections to assess the extent of peribronchiolar and perivascular inflammation in *Il10^{-/-}* and *Il10^{+/+}* mice. We performed immunostaining for cellular proliferation using an anti-Ki67 antibody. We compared Ki67 staining between *Il10^{+/+}* and *Il10^{-/-}* mice in response to air and O₃ in peribronchiolar, perivascular, and centriacinar areas of inflammation.

Real-time quantitative reverse transcriptase-polymerase chain reaction (qRT-PCR). We used the ABI 7000 Sequence Detector (Applied Biosystems, Foster City, CA) to detect IL-10, TNF- α , SOCS3, iNOS, CTSE, WD repeat and FYVE domain containing 1 (WDFY1), SAA3, and S100 calcium binding protein A14 (S100A14) gene expression using gene specific TaqMan qPCR Gene Expression Assays (Applied Biosystems) and Power Syber primer sets (RealTime Primers, LLC, Elkins Park, PA).

Western blot analysis. We subjected aliquots of total proteins (30-80 μ g) to Western blot analyses with specific primary antibodies for CD86 (SC-19617; Santa Cruz Biotechnologies, Santa Cruz, CA), actin (SC-1615, Santa Cruz), phosphorylated STAT3-tyr 701 (Cell Signaling, Danvers, MA), and STAT3 (Cell Signaling). We detected blots using SuperSignal West Pico Chemiluminescent Substrate (Pierce, Rockford, IL) and BioMaxMR x-ray film (Kodak, Rochester, NY). We quantitated the intensity of Western blot bands (Bio-Rad Gel Doc 2000 System, Hercules, PA).

Enzyme-linked immunosorbant assay (ELISA) for MIP-2 and p65 NF- κ B. We processed all samples in duplicate, and absorbance was measured at 450 nm (Benchmark Microplate Reader, Bio-Rad). The minimum detectable level of murine MIP-2 was less

than 1.5 pg/mL. To analyze specific binding activity of nuclear p65 NF- κ B proteins, we performed transcription factor ELISA using nuclear extracts (5 μ g) following the manufacturer's instruction (NF- κ B TransAM kit, Active Motif, Carlsbad, CA) and procedures described previously (Cho et al., 2005).

Nuclear protein isolation and electrophoretic mobility shift assay (EMSA) for NF- κ B. We incubated an aliquot (5 μ g) of nuclear protein in a binding buffer (10mM Tris, pH 7.5, 50 mM NaCl, 1 mM EDTA, 5 % glycerol, 1 mM DTT, 0.2 μ g PolydI-dC, 1 mM PMSF) in a total volume of 19 μ l for 15 min on ice. We then incubated the reaction with 1 μ l of [γ ³²P] dATP end-labeled oligonucleotide containing a NF- κ B consensus sequence (3×10^4 cpm) at room temperature. After 30 min, we subjected the mixture to electrophoresis on a 4% SDS-PAGE gel with 0.25X TBE buffer. We autoradiographed the gels at -70° C. To analyze specific binding activity of NF- κ B subunits, we pre-incubated nuclear proteins (5 μ g) with 4 μ g of anti-p50 NF- κ B antibody (sc-1190X; Santa Cruz), and processed them for gel shift assay as described above.

RNA isolation and microarray hybridization. We harvested the left lobes of mouse lung tissue and the lobes were flash frozen in liquid nitrogen and stored at -80°C. For RNA extraction, we homogenized the lung tissue in 2ml Trizol (Invitrogen, Calsbad, CA) with a Tekmar Tissumizer and saw-tooth generator. We subsequently processed one ml of homogenate according to the manufacturer's (Invitrogen) protocol with the following minor modifications. We used two μ l of 5 mg/ml glycogen as a carrier for the isopropanol precipitation, we increased the duration of the isopropanol precipitation to overnight, and we increased all centrifugation times to 15 minutes. We resuspended RNA pellets in nuclease-free water. We tested RNA quality using a Beckman DU680 spectrophotometer, and we determined quality assessment by RNA Nano LabChip analysis on an Agilent Bioanalyzer 2100. We subsequently performed A Qiagen RNeasy

total RNA cleanup protocol followed by re-quantitation by spectrophotometry. We synthesized double stranded cDNA from 4 μ g of total RNA using the GeneChip Expression 3' amplification reagents one-cycle cDNA synthesis kit (Affymetrix). We column-purified the resultant double-stranded cDNA using the GeneChip Sample Cleanup Module. We synthesized biotinylated cRNA from the double-stranded cDNA by *in vitro* transcription (IVT) using the GeneChip Expression 3' amplification reagents for IVT labeling (Affymetrix), and subsequently purified cRNA by column purification with the GeneChip Sample Cleanup Module (Affymetrix), and quantified the cRNA. We assessed quality of biotinylated cRNAs by RNA Nano LabChip analysis on an Agilent Bioanalyzer 2100. We used a fragmentation buffer (250mM Tris acetate pH 8.1, 150 mM MgOAc, 500mM KOAc) to fragment 15 μ g of cRNA. We then hybridized the fragmented cRNA to GeneChips (Affymetrix Mouse Genome 430A 2.0).

Gene expression analysis. The following section describes the process by which genes were identified for pathway analysis, based on microarray data from RNA isolated from *Il10*^{+/+} and *Il10*^{-/-} mice exposed to filtered air or 0.3 ppm O₃ for 24, 48, or 72 hrs continuously (further details in Materials and Methods). We were interested in finding genes with expression differences in the air and O₃ treatments related to the *Il10* status of the mice.

We used a visual data mining approach to identify candidate probe sets. We first clustered the probe sets based on their expression profiles in all treatments in both strains. This did not yield a meaningful set of profiles; expression differences between the two strains were less pronounced than treatment-related expression differences.

Next we identified treatment-related expression patterns in the *Il10*^{+/+} mice alone, i.e. without including *Il10*^{-/-} mice. Three such patterns are shown in Supplemental Material, Figure 1. Each panel shows a cluster identified using k-means clustering, with

the expression profile closest to the cluster centroid in a darker color, and other profiles in the same cluster in lighter blue.

Selection of profiles to use as seeds for similarity searches

We then explored the expression profiles of these same probe sets in the microarrays from *Il10*^{-/-} animals to identify differences in expression between the two strains. This is summarized in Supplemental Material, Figures 2 – 4. In these Figures, we show clusters of expression profiles identified by k-means clustering. In each case the profile nearest the cluster centroid is shown in bold and the other profiles are shown in a lighter color. This permits assessment of the main pattern in the cluster and also permits a visual estimation of the number of profiles with correlated expression pattern and the degree of correlation. These parameters are used to identify profiles common to groups of more than 10 probe sets, thus profiles suggestive of a common response by a number of probe sets. Once these probe sets are identified, analysis of their biology can identify probe sets with related biological function (suggesting a biological expression response) or those with unrelated function (suggestive either of novel gene response or technical artifact underlying the response).

Panel A, Supplemental Material, Figure 2 redraws the expression profiles in pattern A from SM Figure 1. Profiles (Panel A, Supplemental Material, Figure 2) have relatively consistent expression in the air-exposed and 24-hour O₃-exposed *Il10*^{+/+} mice. Expression profiles increased with additional time in O₃ in *Il10*^{+/+} mice. Panel B of Supplemental Material, Figure 2 shows 25 clusters of these same probe sets in the samples from *Il10*^{-/-} mice. In this case the patterns of expression are qualitatively similar in the *Il10*^{+/+} (Panel A) and *Il10*^{-/-} mice (Panel B). The increase following O₃ exposure may be higher or lower in the *Il10*^{-/-} than in *Il10*^{+/+} for some probe sets, however the trend appears to be the same.

Panel A, Supplemental Material, Figure 3 redraws the expression profiles in pattern B from Supplemental Material, Figure 1. Again, expression profiles are lower in air and 24 hours of O₃ and increase in response to increased O₃ exposures in the *Il10*^{+/+}

animals. However, the increase in expression is not as marked in these profiles as the set shown in Panel A of Supplemental Material, Figure 2. Panel B, Supplemental Material, Figure 3 shows the patterns for these same probe sets in the *Il10*^{-/-} mice. In this set there are two qualitatively different responses seen in the *Il10*^{-/-} mice. Profiles ringed with magenta (6, 10, and 20) appear to increase at 24 hours in the *Il10*^{-/-} mice but were increased at 48 hours in the *Il10*^{+/+} mice. Profiles ringed in green (21 and 25) appear to have similar response kinetics, as expression increases were observed at 48 hours in both *Il10*^{+/+} and *Il10*^{-/-} samples.

Supplemental Material, Figure 4 redraws the expression profiles from pattern C of Supplemental Material, Figure 1. This pattern illustrates those expression profiles which did not change in the *Il10*^{+/+} samples in response to O₃ exposure. With the exception of clusters 3 and 8 (outlined in magenta in the Figure), these profiles are also non-responsive to O₃ in the *Il10*^{-/-} mice across replicate samples.

Similarity searches and results

We used the following profiles as seeds in similarity searches to identify probe sets with correlated expression patterns: (A) The centroid profile in Supplemental Material, Figure 2, panel A was used in order to identify responses to O₃ that were qualitatively similar in both strains; or (B) the centroids of clusters outlined in magenta in Supplemental Material, Figures 3 and 4 (responses qualitatively different in *Il10*^{+/+} and *Il10*^{-/-} mice). Similarity searches used cosine correlation as a metric, and selected profiles had a similarity threshold of r = 0.9856.

Similarity searches led to 357 probe sets. We found a small number of probe sets with higher expression in *Il10*^{-/-} compared to *Il10*^{+/+} mice independent of treatment (Supplemental Material, Figure 5, Panel C) and two probe sets with erratic expression (not shown). However, the majority of profiles increased after exposure to O₃, either with similar kinetics in *Il10*^{-/-} and *Il10*^{+/+} mice (panels A and B of Supplemental Material, Figure 5), or with an apparent delay in the *Il10*^{+/+} mice compared to the *Il10*^{-/-} mice (Panel D of Supplemental Material, Figure 5).

Identification of responsive genes

The probe sets were combined on the basis of gene and pattern using the following rule: if a gene (identified by UniGene ID) was represented by more than one probe set, then one probe set was selected as a representative of the locus unless the probe sets had different expression patterns. In four cases the patterns were different between the two probe sets. In these cases, the patterns were related to treatment, but one fell into the “small change in intensity” category (Panel B of Supplemental Material, Figure 5) and one had a larger change; in these four cases we used the pattern with the larger difference to classify the gene. If the gene had more than two probe sets then the pattern seen most frequently was selected. There were five sets of genes with multiple probe sets all with the same profile; three sets where some probe sets were classified as the pattern in panel A of Supplemental Material, Figure 5 and others as the pattern in Panel B, and one set where the probe sets were classed as the patterns in panels B or D. In this last case we selected the majority pattern to use to classify the gene. The resulting 165 genes and annotations are given in Tab “165 genes” of Supplemental Material, Table 2. Those which had multiple probe sets are indicated in the column headed “multiple probes”.

Pathway identification of genes with responsive profiles

Tab “DAVID” of Supplemental Material, Table 2 illustrates the results from analysis using DAVID (**D**atabase for **A**nnotation, **V**isualization and **I**ntegrated **D**iscovery 2008). The majority of the pathways identified as enriched by DAVID in our gene list were related to cell cycle and DNA replication. These pathways suggested altered cell cycle kinetics rather than providing insight into the underlying biology. The list of 165 genes was then loaded into Ingenuity Pathway Analysis version 7.4 (IPA, April, 2009) tool for alignment with the literature. Three sets of genes were loaded, and labeled according to their profile in Supplemental Material, Figure 5 (see Supplemental Material, Table 2, Tab “165 genes”, column SM, Fig 5/IPA). Genes with profiles shown in Panel A were coded red, those with profiles in Panel B were coded yellow, and those with profiles in Panel D were coded green. Note that the color does not correspond to

expression level but to overall profile pattern. This was done so that the genes with different response patterns could be compared. The top three networks identified in IPA are given in Supplemental Material, Table 3. Networks with a score below 30 for mice can include interactions we deem to be of low significance (unpublished); so we use a score of 30 as a cutoff for IPA analysis of mouse microarray data. The top networks with scores above 30 are described in Supplemental Material, Table 3, and provide the basis for Figure 4 in the manuscript.

Analysis of microarray data using GeneSpring

The array expression files (CEL) were transferred to GeneSpring GX 11.0 Expression Analysis software program (Agilent Technologies, Inc., Santa Clara, CA) for statistical analyses. Intensity of each gene on GeneChip triplicates per group was first normalized to the mean intensity of the same gene in *Il10*^{+/+} air group. These relative expression ratios were analyzed by 2-way ANOVA ($p < 0.01$) without multiple comparison corrections using genotype (*Il10*^{+/+}, *Il10*^{-/-}) and exposure (air, 24 h O₃, 48 h O₃, 72 h O₃) as the variables to determine the effect of O₃ on gene expression kinetics between *Il10*^{+/+} and *Il10*^{-/-} mice. These analyses elucidated 453 genes significantly altered by O₃ in an IL-10-dependent manner (see Supplemental Material, Table 4 and Figure 6). We then further filtered these genes to include only those with expression changes 2-fold greater or 2-fold less than air-exposed *Il10*^{+/+} mice and these genes are listed in Supplemental Material, Table 4.

References

Cho HY, Jedlicka AE, Clarke R, Kleeberger SR. 2005. Role of toll-like receptor-4 in genetic susceptibility to lung injury induced by residual oil fly ash. *Physiol Genomics* 16(22):108-117.

Supplemental Material, Table 1.

Exposure	Genotype	Total Cells ^a	Macrophages ^a	Lymphocytes ^a	Epithelial Cells ^a
Air	<i>Il10</i> ^{+/+}	43.83 ± 4.39	42.17 ± 4.19	0.04 ± 0.02	1.55 ± 0.24
	<i>Il10</i> ^{-/-}	39.89 ± 2.82	40.88 ± 4.49	0.02 ± 0.01	1.74 ± 0.17
24 h O ₃	<i>Il10</i> ^{+/+}	42.33 ± 5.81	75.96 ± 19.41	0.02 ± 0.01	4.11 ± 1.17
	<i>Il10</i> ^{-/-}	75.00 ± 4.34*	38.83 ± 2.73	0.0 ± 0.0	1.72 ± 0.36
48 h O ₃	<i>Il10</i> ^{+/+}	75.00 ± 11.26	75.63 ± 13.04	0.12 ± 0.06	3.36 ± 1.01
	<i>Il10</i> ^{-/-}	124.20 ± 33.39*	64.11 ± 8.27	1.23 ± 0.46	2.51 ± 1.16
72 h O ₃	<i>Il10</i> ^{+/+}	80.33 ± 4.81	116.48 ± 23.61	0.01 ± 0.00	3.05 ± 0.92
	<i>Il10</i> ^{-/-}	173.40 ± 34.16*	128.43 ± 29.56	0.06 ± 0.05	1.72 ± 0.40

^aAll cell numbers are x10³. * p < 0.05, compared to *Il10*^{+/+} mice.

Supplemental Material, Table 1. Effect of targeted deletion of *Il10* on the total cells and specific inflammatory cell types (macrophages, lymphocytes, epithelial cells) recovered in the BALF from *Il10*^{+/+} and *Il10*^{-/-} mice in response to air or 0.3 ppm O₃.

Supplemental Material, Table 2 is provided as a separate Excel file.

Supplemental Material, Table 2. Tab 1: “165 genes”. List of genes identified by visual data mining, organized into specific pattern identities. Indications as to multiple probe sets and the name of the representative probe set are included. Additional columns include gene abbreviations, gene names, gene functions, chromosomal locations, and database links to SWISSPROT, GENE ONTOLOGY, and ENTREZ GENE. Columns also include RMA-normalized data used to detect gene expression patterns. Tab 2: “DAVID” (Database for Annotation, Visualization and Integrated Discovery, <http://david.abcc.ncifcrf.gov/>; GO January 2008 version) gene categories, terms, count, P-values, fold-enrichment, Bonferroni, Benjamini, and false discovery rate (FDR) values for array analyses.

Supplemental Material, Table 3. Networks with Score above 30 in IPA (v 7.4, April 2009).

ID	Score	Genes	Top Functions
1	58	29	Infectious Disease, Inflammatory Disease, Neurological Disease
2	53	27	DNA Replication, Recombination and Repair, Cancer, Gastrointestinal Disease
3	34	19	Tissue Development, Drug Metabolism, Lipid Metabolism

Supplemental Material, Table 3. IPA Networks with Score above 30 in IPA. The Table provides the three top IPA scores, the number of genes in the network that were identified via our analysis, and the top functions associated with those genes. These networks are represented graphically in manuscript Figure 4.

Supplemental Material, Table 4 is provided as a separate Excel file.

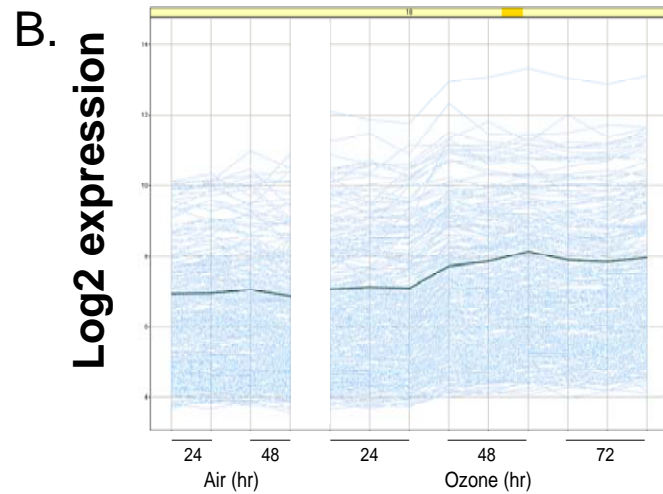
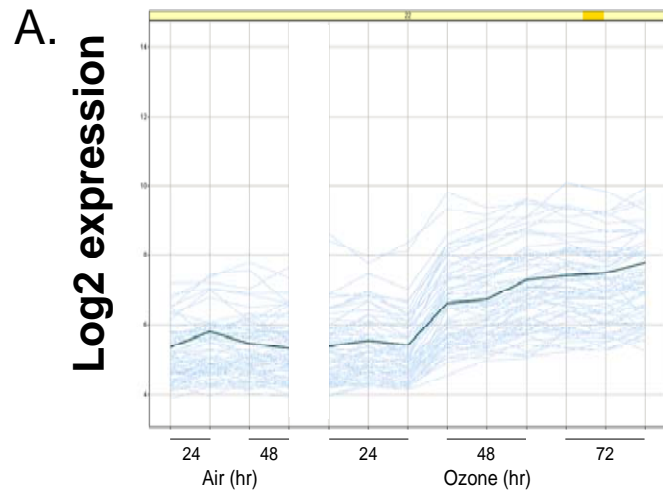
Supplemental Material, Table 4. Genes that were expressed differentially between *Il10*^{+/+} and *Il10*^{-/-} mice in response to O₃. Gene transcripts were initially filtered by 2-way ANOVA analysis (p<0.01) using GeneSpring. The transcripts were then further filtered to include only those that were 2-fold greater or 2-fold less than those in air-exposed *Il10*^{+/+} and *Il10*^{-/-} mice in response to O₃. Genes that were identified using visual mining and GeneSpring analyses are highlighted in yellow.

Supplemental Material Figure Legends

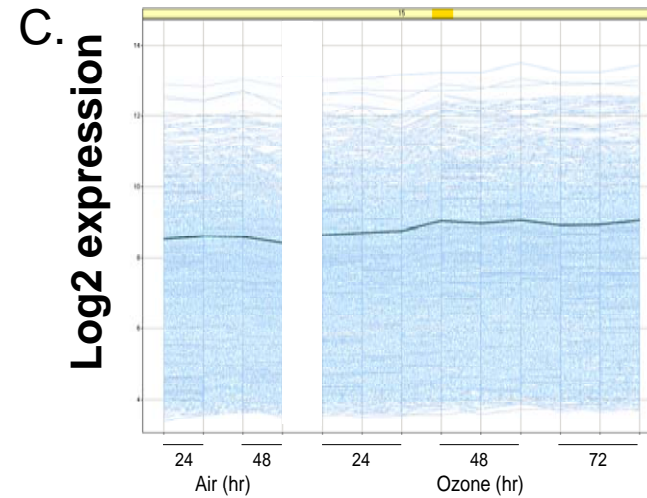
Supplemental Material, Figure 1. Expression profiles in air- and O₃-exposed *Il10*^{+/+} mice. Dark line is the profile at cluster centroid, other correlated profiles are in light blue.

Supplemental Figure 1.

Profiles with increased expression following exposure to ozone



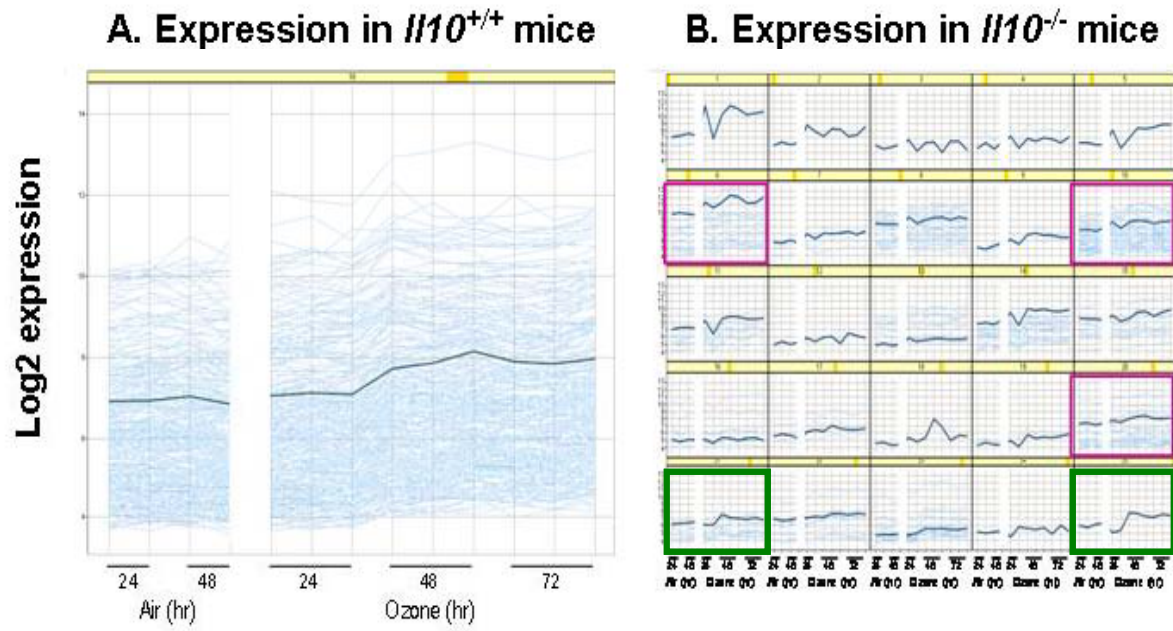
Example of profiles which do not respond to ozone exposure



Supplemental Material, Figure 2. Expression profiles with Supplemental Material, Figure 1, pattern A in air- and O₃-exposed *Il10*^{+/+} mice. Dark line represents the cluster centroid; other correlated profiles are in light blue. Panel A (Supplemental Material, Figure 2) shows the expression profile in *Il10*^{+/+} mice, panel B (Supplemental Material, Figure 2) shows comparative expression profiles in *Il10*^{-/-} mice. Panel B shows an array of 25 graphs corresponding to the different patterns detected across *Il10*^{-/-} mice. Each graph in Panel B has the same axes as the larger graph in Panel A.

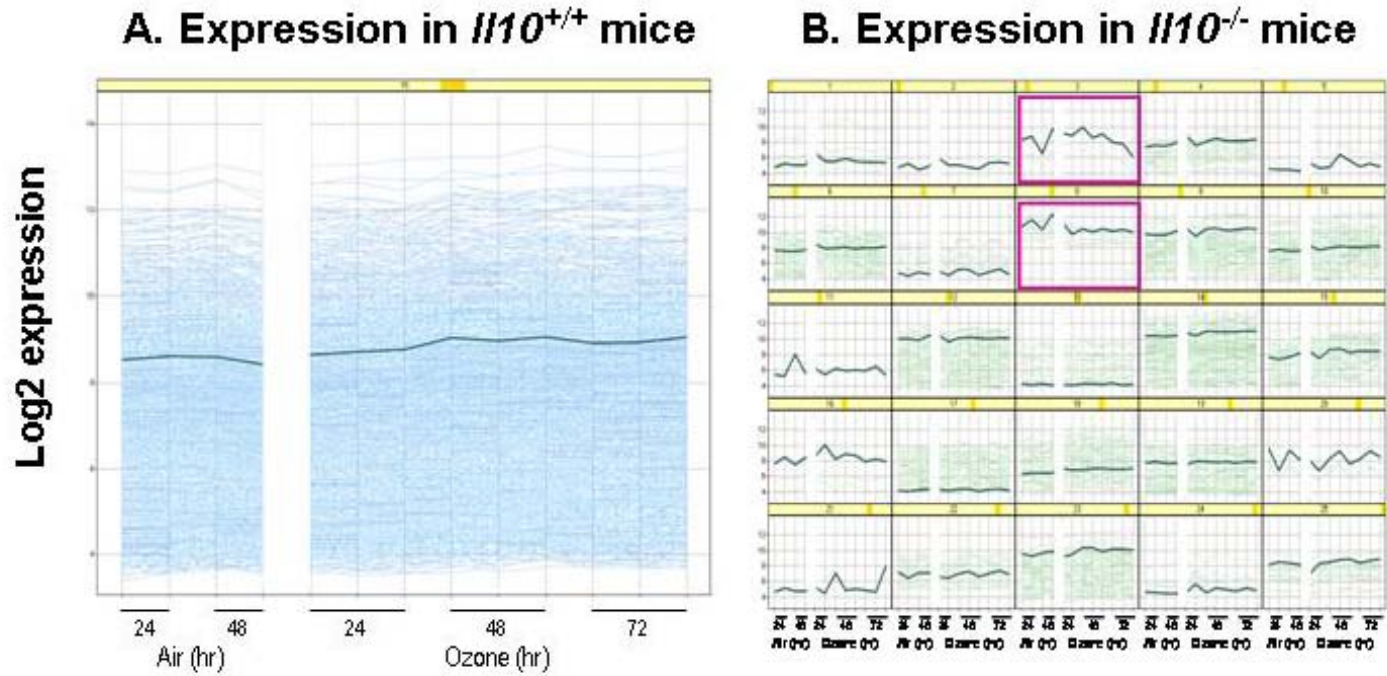
Supplemental Material, Figure 3. Expression profiles with Supplemental Material, Figure 1, pattern B in air- and O₃-exposed *Il10*^{+/+} mice. The dark line represents the profile at the cluster centroid; other correlated profiles are in light blue. Panel A illustrates the expression profile in *Il10*^{+/+} mice. Panel B shows an array of 25 graphs corresponding to the different patterns detected in the *Il10*^{-/-} specimens. Each graph in Panel B has the same axes as the larger graph in Panel A. Green boxes in Panel B indicate patterns in *Il10*^{-/-} mice that are similar to expression patterns in *Il10*^{+/+} mice; magenta boxes indicate qualitatively different expression patterns between *Il10*^{+/+} and *Il10*^{-/-} mice.

Supplemental Figure 3.



Supplemental Material, Figure 4. Expression profiles with Supplemental Material, Figure 1, pattern C in air- and O₃-exposed *Il10*^{+/+} mice. The dark line represents the profile at the cluster centroid; other correlated profiles are in light blue. Panel A shows expression profile in *Il10*^{+/+} mice. Panel B shows an array of 25 graphs corresponding to the different patterns detected in the *Il10*^{-/-} specimens. Each graph in Panel B has the same axes as the larger graph in Panel A. Magenta boxes indicate qualitatively different expression patterns between *Il10*^{+/+} and *Il10*^{-/-} mice.

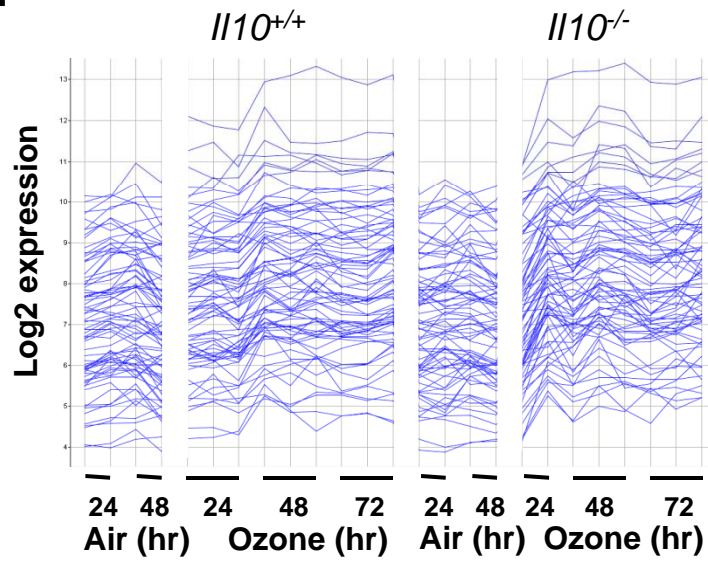
Supplemental Figure 4.



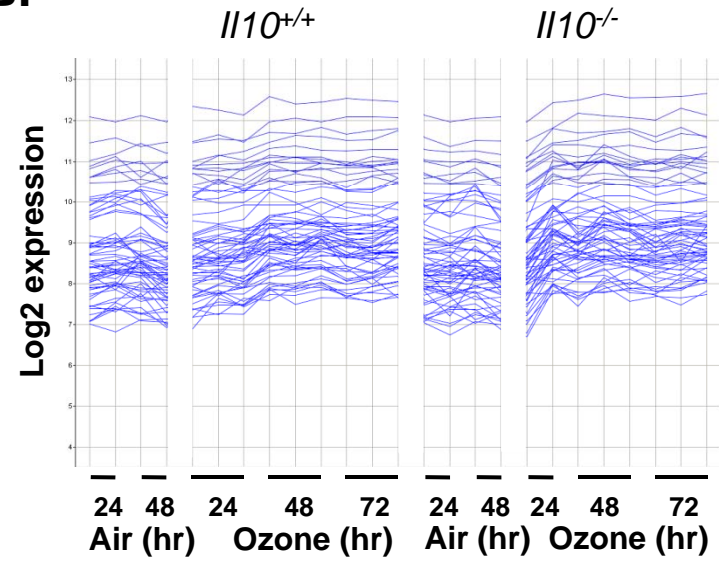
Supplemental Material, Figure 5. Profiles resulting from similarity searches. Panels A and B – response to O₃ with similar expression profiles in *Il10*^{+/+} and *Il10*^{-/-} mice: Panel A represents the “larger change in intensity” between air and O₃ exposure, while Panel B represents a “smaller change in intensity” between air and O₃ exposure. Panel C represents a “higher response in *Il10*^{-/-} than in *Il10*^{+/+}”; all but two profiles are essentially unaffected by O₃ exposure. Panel D illustrates responses to O₃ exposure that were altered temporally between *Il10*^{-/-} and *Il10*^{+/+} mice.

Supplemental Figure 5.

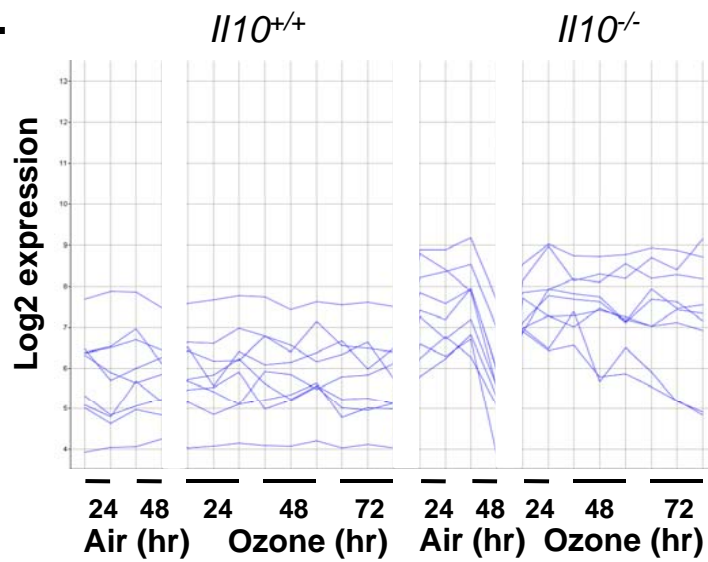
A.



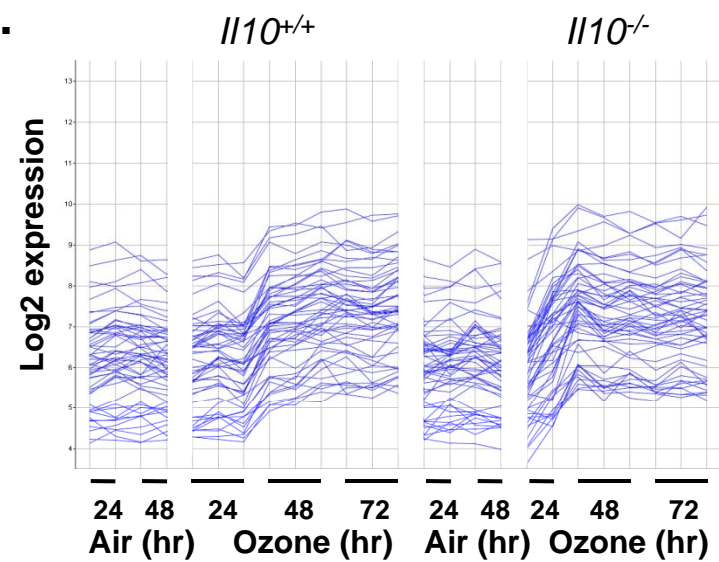
B.



C.

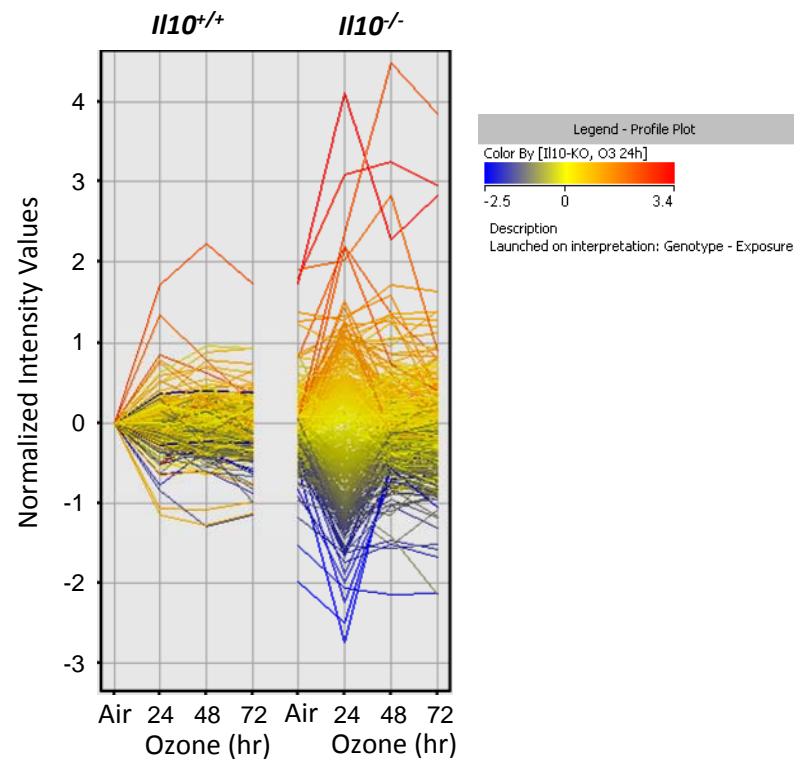


D.



Supplemental Material, Figure 6. Expression profiles of 453 genes significantly varied between *Il10*^{+/+} and *Il10*^{-/-} mice in response to O₃: GeneSpring analysis determined 453 genes expressed significantly differently between *Il10*^{+/+} and *Il10*^{-/-} mice during 24-72 h O₃ exposure. Expression level of each gene was normalized to that of air-exposed *Il10*^{+/+} mice and was expressed as relative log₂ ratio. Color bar is the indicator of expression intensity.

Supplemental Figure 6.



Supplemental Material, Figure 7. Validation of microarray analysis for four genes that were differentially expressed in *Il10*^{+/+} and *Il10*^{-/-} mice: cathepsin E (*Ctse*), WD repeat and FYVE domain containing 1 (*Wdfy1*), serum amyloid A 3 (*Saa3*), and S100 calcium binding protein A14 (*S100a14*). We processed total lung RNA from *Il10*^{+/+} and *Il10*^{-/-} mice utilized for microarray analysis for qRT-PCR analysis to confirm expression profiles of the genes elucidated by unsupervised (SpotFire) and supervised (GeneSpring) analysis. PCR results are presented as relative band intensities compared with air-exposed *Il10*^{+/+} mice. Data are presented as means ± SE (n=3 per group). *, significantly different from genotype-matched air control mice ($p < 0.05$). +, significantly different from exposure-matched *Il10*^{+/+} mice ($p < 0.05$).

Supplemental Figure 7.

